



Chromium(VI) removal by maghemite nanoparticles

Wenjun Jiang^a, Miguel Pelaez^b, Dionysios D. Dionysiou^b, Mohammad H. Entezari^{c,*}, Dimitra Tsoutsou^d, Kevin O'Shea^{a,*}^a Department of Chemistry and Biochemistry, Florida International University, Miami, FL 33199, USA^b Environmental Engineering and Science Program, University of Cincinnati, Cincinnati, OH 45221-0012, USA^c Department of Chemistry, Ferdowsi University of Mashhad, Mashhad 91775, Iran^d Institute of Advanced Materials, Physicochemical Processes, Nanotechnology and Microsystems (IAMPPNM), National Center for Scientific Research "Demokritos", 153 10 Aghia Paraskevi Attikis, Athens, Greece

H I G H L I G H T S

- ▶ Co-precipitation synthesis of maghemite nanoparticles.
- ▶ The adsorption of Cr(VI) follows a pseudo-second-order kinetic model.
- ▶ The adsorption of Cr(VI) occurs in two phases.
- ▶ Accurate modeling using Langmuir and Langmuir–Freundlich isotherms.
- ▶ Solution pH and presence of humic acid influence adsorption.

A R T I C L E I N F O

Article history:

Received 13 November 2012

Received in revised form 15 February 2013

Accepted 17 February 2013

Available online 24 February 2013

Keywords:

Maghemite nanoparticles

Chromate

Adsorption isotherm

Kinetic study

pH effect

Humic acid

A B S T R A C T

Maghemite nanoparticles were prepared by a co-precipitation method and characterized by Fourier transform infrared spectroscopy, transmission electron microscopy, X-ray photoelectron spectroscopy, nitrogen adsorption and desorption isotherms. The Brunauer–Emmett–Teller surface area, average particle size, pore volume and porosity of maghemite were $73.8 \text{ m}^2 \text{ g}^{-1}$, $17.2 \pm 4.4 \text{ nm}$, $0.246 \text{ cm}^3 \text{ g}^{-1}$, and 56.3%, respectively. Removal of Cr(VI) by the maghemite nanoparticles follows a pseudo-second-order kinetic process. Intraparticle diffusion kinetics implies the adsorption of Cr(VI) onto the maghemite occurs via two distinct phases: the diffusion controlled by external surface followed by an intra-particle diffusion. The equilibrium data was nicely fit to the Langmuir and Langmuir–Freundlich (L–F) models and indicates the adsorption of Cr(VI) is spontaneous and highly favorable. The heterogeneity index, 0.55, implies heterogeneous monolayer adsorption. The adsorption of Cr(VI) is favorable under acidic and neutral conditions with maximum removal observed at pH 4. The adsorption of Cr(VI) is modestly inhibited by the presence of ≥ 5 ppm humic acid. In summary, the adsorption of Cr(VI) by maghemite nanoparticles is rapid, can be accurately modeled, and is effective under a variety of conditions. Our results indicate these magnetic materials have promising potential to cleanup Cr(VI) contaminated waters to acceptable drinking water standards.

© 2013 Elsevier B.V. All rights reserved.

1. Introduction

Chromium is a common drinking water contaminant in the USA because of its wide spread use in industrial processes [1]. The use of chromium in wood preservatives, leather tanning, paint formulation, steel fabrication, and metal finishing are the main sources of chromium based pollution. The toxicity and mobility of chromium

are strongly dependent on the oxidation state. In nature, chromium exists primarily in two oxidation states (III and VI). Cr(III), an essential trace element for human beings, may play a role in the metabolism of glucose [2]. Cr(VI) is a more toxic and soluble specie, compared to Cr(III) which is toxic only at a high concentrations. CrO_4^{2-} and $\text{Cr}_2\text{O}_7^{2-}$ are the primary forms of Cr(VI) with $\text{Cr}_2\text{O}_7^{2-}$ being predominant under strongly acidic conditions and at high Cr(VI) concentrations in aqueous solutions [3]. Cr(VI) is a human carcinogen and poses a significant threat to the environment and human beings [4]. The World Health Organization (WHO) recommends a maximum allowable level of 50 ppb total chromium for drinking water. The US Environmental Protection Agency

* Corresponding authors. Tel.: +1 305 348 3968 (K. O'Shea), tel.: +98 511 8797022x306 (M.H. Entezari).

E-mail addresses: moh_entezari@yahoo.com (M.H. Entezari), osheak@fiu.edu (K. O'Shea).

established a guideline of 100 ppb maximum contaminant level for total chromium in drinking water [5], while California's office of Environmental Health Hazard Assessment proposed in 1999 a public health goal of ≤ 2.5 ppb for total chromium [6].

Unlike many organic pollutants, chromium species are not removed and/or degraded through typical environmental and biological processes, thus it is critical to develop and identify an effective method for the removal of chromium from industrial wastewater. Water purification technologies must be capable of reducing the level of chromium considered safe for human consumption. A number of conventional methods have been employed for the removal of Cr(VI) from wastewater [7]. Adsorption processes can offer significant advantages including availability, profitability, ease of operation and efficiency, in comparison with many conventional methods. A variety of natural and synthetic materials have been used as Cr(VI) sorbents, including activated carbons, biological materials, zeolites, chitosan, and industrial wastes. Unfortunately, these sorbents can also suffer from a number of disadvantages, including high cost, low adsorption capacity and/or difficulties associated with separation and removal following treatment. The application of magnetic nanoparticles for adsorption is attractive because of their high surface area, easy separation and recovery [8,9]. Iron based materials are especially attractive because they are inexpensive and environmentally friendly [10,11]. The magnetite form of iron can be oxidized to maghemite under aerated conditions [12]. Maghemite, a common magnetic material, is a promising adsorbent for heavy metals removal because it is inexpensive, readily available and can be easily separated and recovered [13,14]. While maghemite nanomaterials appear to be promising for Cr(VI) removal, detailed kinetic and adsorption studies have yet to be reported. Herein we report the synthesis of maghemite nanoparticles by a co-precipitation method. The observed adsorption of Cr(VI) by maghemite nanoparticles is rapid, accurately model and effective under a variety of conditions. Our results demonstrate these maghemite nanoparticles with high adsorption capacity and magnetic properties are promising materials for the Cr(VI) removal from aqueous solution.

2. Materials and methods

2.1. Materials

Trace metal grade nitric acid, sodium hydroxide, ferric chloride hexahydrate, ferrous chloride tetrahydrate, 29% ammonium hydroxide and ethanol were purchased from Fisher. Potassium chromate was obtained from Mallinckrodt. Humic acid was obtained from Fluka. All the chemicals were used without further purification. All the solutions were prepared with Millipore filtered water (18 M Ω cm).

2.2. Preparation of maghemite

All solutions were purged with argon for 15 min to remove oxygen prior and during reaction. Iron solutions of FeCl₂·4H₂O (2.0 g) and FeCl₃·6H₂O (5.4 g) were diluted to 30 mL with water. The iron mixture was stirred magnetically, gently purged with argon and heated to 80 °C and then 40 mL of 15% diluted ammonium hydroxide solution added dropwise into the mixture over a 20 min time interval. The mixture was aged at 80 °C for an additional 40 min. The product was rinsed with water then ethanol three times. The samples were separated using a magnet and dried in a vacuum oven at 50 °C to a constant weight [15].

2.3. Characterization

The dried maghemite samples from a single batch were used for adsorption experiments and characterization using XPS, FTIR and TEM. TEM was used for measurement of the average size. The Fourier transform infrared spectroscopy (FTIR) spectra were collected using a Perkin–Elmer spectrum 100 FTIR spectrometer. Transmission electron microscopy (TEM) was carried out using a Philips CM20 with field emission gun at 200 kV and energy dispersive analysis X-ray (EDAX). X-ray photoelectron spectroscopy (XPS) was determined using a PHI 5000 VersaProbe with Al K α radiation (1486.6 eV) at a takeoff angle at 45°. The binding energies were referenced to the C1s core level at 284.8 eV. Nitrogen adsorption and desorption isotherms were performed on a Tristar 300 (Micromeritics) porosimeter analyzer. The sample was prepared by purging with nitrogen gas at 150 °C for 2.0 h using a Flow Prep 060 (Micromeritics) before analysis.

2.4. Adsorption tests

Volumetric glassware was used in the preparation and transfer of all Cr(VI) solutions. Maghemite particles were added to 200 mL Cr(VI) solutions at the desired concentration in a 250 mL Erlenmeyer flask. The experiments were carried out on an orbit shaker (Lab-line instrument Inc., model 3520) with continual mixing at 300 RPM at ~ 25 °C in a temperature controlled laboratory. Five mL of sample were taken at the specific time intervals and filtered through a 0.45 μ m PTFE filter immediately to remove the suspended particles. To the filtrates, nitric acid was added to yield a nitric acid concentration of 0.2% prior to analysis. The concentration of chromium was measured using a Perkin–Elmer AA600 atomic absorption spectrophotometer. The current was 25.0 mA, with the wavelength of detection set at 357.9 nm and slit bandwidth of 0.7 nm as recommended by the manufacturer. Sample concentrations were determined based on a calibration of the instrument in the range from 1 to 50 ppb of chromium. The reproducibility based on representative triplicate runs was $\pm 5\%$.

3. Results and discussion

3.1. Characterization

FTIR analysis was employed to determine specific functionality of the nanoparticles. The most abundant functional group observed in our samples of maghemite was the hydroxyl group with a broad band at 3300 cm⁻¹ (OH stretching mode), and bands at 1625.3 and 1428.2 cm⁻¹ (OH bending modes). The Fe–O stretching bands appear at 539.2 and 526.8 cm⁻¹ [16]. The TEM image of maghemite shows the average size of synthesized maghemite particle is 17.2 \pm 4.4 nm. The EDAX analysis showed the particles contained 31.28% O, 1.75% C and 66.97% Fe (wt%).

The Brunauer–Emmett–Teller (BET) surface area, pore volume, porosity, Barret–Joyner–Halenda (BJH) pore size and distribution were obtained from nitrogen adsorption and desorption isotherms. The nitrogen adsorption and desorption isotherms are showed in Fig. 1 with a characteristic type H3 hysteresis loop. The BJH pore size distribution was inserted in Fig. 1, and a sharp peak appears at 13.28 nm. The BET surface area, pore volume and porosity are 73.8 m² g⁻¹, 0.246 cm³ g⁻¹, 56.3%, respectively. The chemical composition was further characterized using XPS. The XPS spectrum is shown in Fig. 2. The predominant elements are Fe and O, and small amounts of residual Cl and C are also present. The peaks at binding energy of 56, 198.3, 284.8 and 530.4 eV were designated for Fe3p_{3/2}, Cl2p, C1s and O1s, respectively. High resolution XPS of Fe2p is inserted in Fig. 2. Binding energy of Fe2p_{1/2} is 724.8 eV

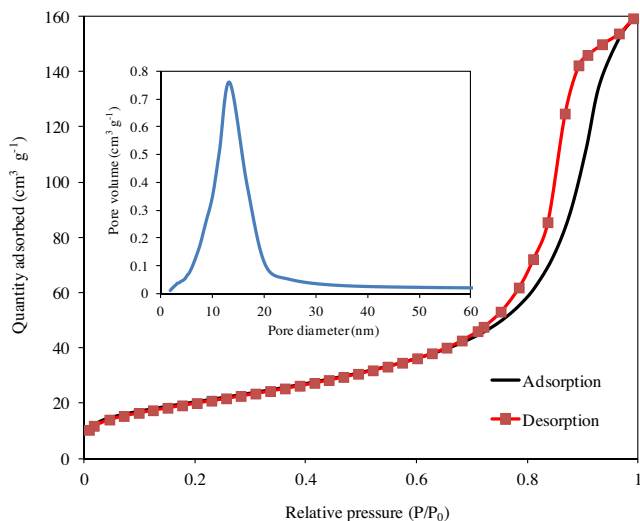


Fig. 1. Nitrogen adsorption and desorption isotherms. The inset is pore size distribution of maghemite particles.

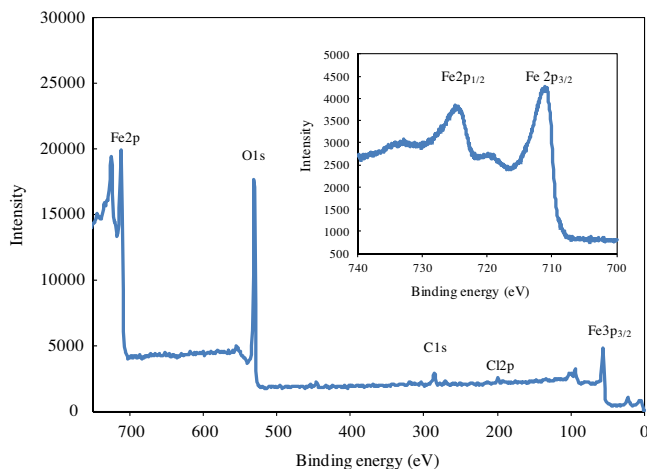


Fig. 2. XPS of maghemite particles and high resolution XPS of Fe2p core level (the inset).

and binding energy of Fe2p_{3/2} is 711.1 eV. The presence of satellite peak at 719 eV is characteristic for maghemite. These results agree with literature values of maghemite particle [17,18]. A multiplet analysis of the Fe2p_{3/2} peak indicates again the sample is maghemite [19].

3.2. Effect of the concentration of maghemite on Cr(VI) adsorption

The Cr(VI) adsorption by maghemite was performed with continuous mixing on an orbit shaker at room temperature and 300 RPM. The Cr(VI) remaining in solution was monitored as a function of maghemite concentration and contact time.

Experiments were run with the initial concentration of Cr(VI) at 500 ppb, while varying the contact time from 0 to 120 min, and initial concentration of maghemite from 0.1 to 1.5 g L⁻¹. The adsorption of Cr(VI) by maghemite particle was rapid in the first 5 min followed by a slow Cr(VI) adsorption stage at longer contact times as illustrated in Fig. 3. At initial maghemite concentrations ≥ 0.3 g L⁻¹, the concentration of Cr(VI) in the aqueous phase was effectively reduced to 100 ppb within 60 min. Under these conditions the concentration of Cr in solution was reduced within the

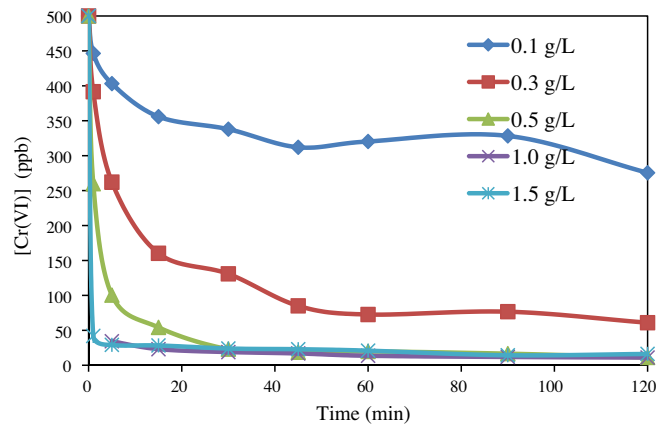


Fig. 3. Effect of the concentration of maghemite particles on Cr(VI) adsorption.

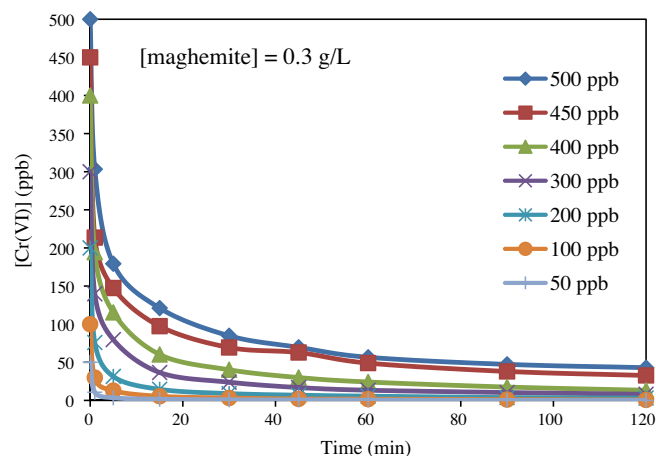


Fig. 4. Effect of the initial concentration of Cr(VI) and contact time on Cr(VI) removal.

drinking water guidelines recommended by EPA. The residual Cr(VI) in solution increased as a function of decreasing concentration of maghemite. Based on the adsorption studies, a concentration of 0.3 g L⁻¹ maghemite was employed for studying the kinetics and equilibrium adsorption isotherms.

3.3. Effect of the initial Cr(VI) concentration and contact time on Cr(VI) adsorption

The concentration of Cr(VI) in the aqueous phase vs. the adsorption time at various initial concentrations of Cr(VI) is illustrated in Fig. 4. The adsorption process is rapid for the first 20 min, followed by a slower uptake. The concentration of Cr(VI) in the aqueous phase at equilibrium gradually increases with increases in the initial concentration of Cr(VI). After 2 h, the observed removal efficiency of Cr(VI) by maghemite at initial Cr(VI) concentration of 50, 100, 200, 300, 400, 450 and 500 ppb were 100%, 99.4%, 98.5%, 97.3%, 96.7%, 92.8% and 91.4%, respectively. Under these experimental conditions, the removal efficiency of Cr(VI) modestly decreased as a function of the increase in initial concentrations of Cr(VI).

3.4. Adsorption kinetic study

3.4.1. Pseudo-second-order model

To further investigate the adsorption of Cr(VI) by co-precipitation prepared maghemite, an adsorption kinetic study was carried

out. Application of pseudo-first order kinetic model to experimental data yielded poor results. With this in mind, we applied the pseudo-second-order equation expressed below [20]:

$$dQ_t/dt = k_p(Q_e - Q_t)^2 \quad (1)$$

where k_p is the rate constant of pseudo-second-order model ($\text{g mg}^{-1} \text{min}^{-1}$), t is the reaction time (min), Q_t is the amount of adsorbate adsorbed per unit mass by maghemite at the specific time (mg g^{-1}), and Q_e is the adsorption capacity at adsorption equilibrium (mg g^{-1}), respectively.

The pseudo-second-order kinetics model nicely simulates the adsorption of Cr(VI) by maghemite and the resulting kinetic parameters are summarized in Table 1. The data indicate the adsorption of Cr(VI) at each specific initial Cr(VI) concentration nicely fits the pseudo-second-order model based on the coefficient of determination (R^2). The mathematical expressions of initial Cr(VI) concentration (C_0 in ppb) vs. k_p and Q_e , and both of with k_p and Q_e are a function of initial Cr(VI) concentration, are expressed in Eqs. (2) and (3). The k_p decreased as the increase of initial Cr(VI) concentration, while Q_e increased linearly. Substituting Eqs. (2) and (3) into Eq. (1) yields Eq. (4), an empirical adsorption kinetics equation. The adsorption rate is a function of C_0 . For a typical second-order kinetic reaction, the rate constants are temperature dependent, and usually follow the Arrhenius equation. However the rate constants decreased with an increase in the initial Cr(VI) concentration. Ofomaja suggested that a chemical activation mechanism occurred during the adsorption process for an analogous behavior for adsorption of methylene blue onto palm kernel fibre [21]. The adsorption is accurately modeled by pseudo-second-order model at a fixed initial Cr(VI) concentration under our experimental conditions.

$$K_p = 22,142 C_0^{-1.838} \quad (2)$$

$$Q_e = 0.0031 C_0 + 0.0294 \quad (3)$$

$$dQ_t/dt = 22,142 \times C_0^{-1.838} \times (0.0031 C_0 + 0.0294 - Q_t)^2 \quad (4)$$

3.4.2. Intraparticle diffusion kinetic model

The intraparticle diffusion kinetic model has also been employed to investigate the adsorption processes [22]. The model is expressed as:

$$Q_t = k_{id}t^{1/2} + C \quad (5)$$

where k_{id} is the intraparticle diffusion rate constant ($\text{mg g}^{-1} \text{min}^{-1/2}$) and C , the intercept represents the thickness of boundary layer effect. There is a positive relationship between the value of C and the boundary layer effect which implies the contribution of surface sorption in the rate controlling step. The intraparticle diffusion plot is given in Fig. 5. If the regression of Q_t against $t^{1/2}$ is linear and the intercept is 0, the adsorption rate was exclusively controlled by intraparticle

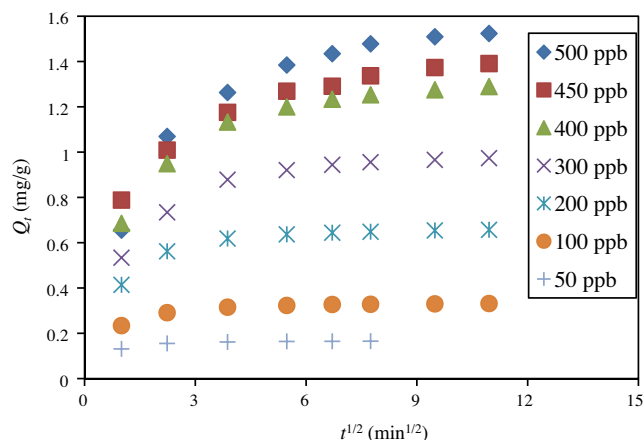


Fig. 5. Intraparticle diffusion plots for removal of Cr(VI) by maghemite particles.

diffusion. As shown in Fig. 5, the intercepts were not zero, indicating surface sorption and intraparticle diffusion are rate controlling processes [23]. The plot suggests that the sorption followed two phases. The first phase is the diffusion controlled by external surface; and the second phase has been assigned to intra-particle diffusion [24].

3.5. Adsorption isotherms

The adsorption of Cr(VI) onto maghemite was evaluated using the Freundlich, Langmuir, L-F and Temkin adsorption isotherms. Each of these models involves variations in the extent and different types of adsorption modes. The details of each model are provided in the following section and plots of the experimental data for models are illustrated in Fig. 6.

Freundlich isotherm assumes that the binding sites on the surface of adsorbent are heterogeneous, the adsorption is more difficult as more and more binding sites are occupied by adsorbates and multilayer adsorption can occur. The Freundlich isotherm [25] can be represented in the following form:

$$Q_e = KC_e^{1/n} \quad (6)$$

where C_e is the equilibrium chromium concentration in solution (mg g^{-1}). K indicates the relative adsorption capacity of the adsorbent and n represents the adsorption intensity. In order to linearize it, the Freundlich isotherm is expressed as:

$$\log Q_e = \log K + 1/n \log C_e \quad (7)$$

The K and n were derived from Fig. 6a. The value of K is 5.20 mg g^{-1} , while n is 2.77. The Freundlich constant, n , can be used to predict the adsorption characteristics. For $n < 1$ the adsorption is considered poor, n between a value of 1 and 2 adsorption is defined as moderately difficult with n values between 2 and 10 is considered good adsorption [26]. The value of $n = 2.77$ determined in our studies represents good adsorption. Our results indicate the removal of chromium with small dosages of maghemite is practical.

Langmuir isotherm equation is derived from the assumption that the adsorbent surface has a fixed number of equivalent binding sites, and the monolayer adsorption occurs without transmigration of adsorbate on the surface of adsorbent isotherm [25]. The data were modeled with Langmuir adsorption isotherm.

$$C_e/Q_e = 1/bQ_m + C_e/Q_m \quad (8)$$

where b and Q_m are the Langmuir adsorption constant (L mg^{-1}) and maximum capacity of adsorbent (mg g^{-1}), respectively. The values

Table 1
Kinetic parameters of pseudo-second-order model for adsorption of Cr(VI) as a function of initial concentration of Cr(VI).

C_0 (ppb)	k_p ($\text{g mg}^{-1} \text{min}^{-1}$)	Q_e (mg g^{-1})
50	17.22	0.166
100	4.01	0.333
200	1.58	0.661
300	0.62	0.984
400	0.38	1.304
450	0.28	1.409
500	0.23	1.551

$R^2 \geq 0.999$

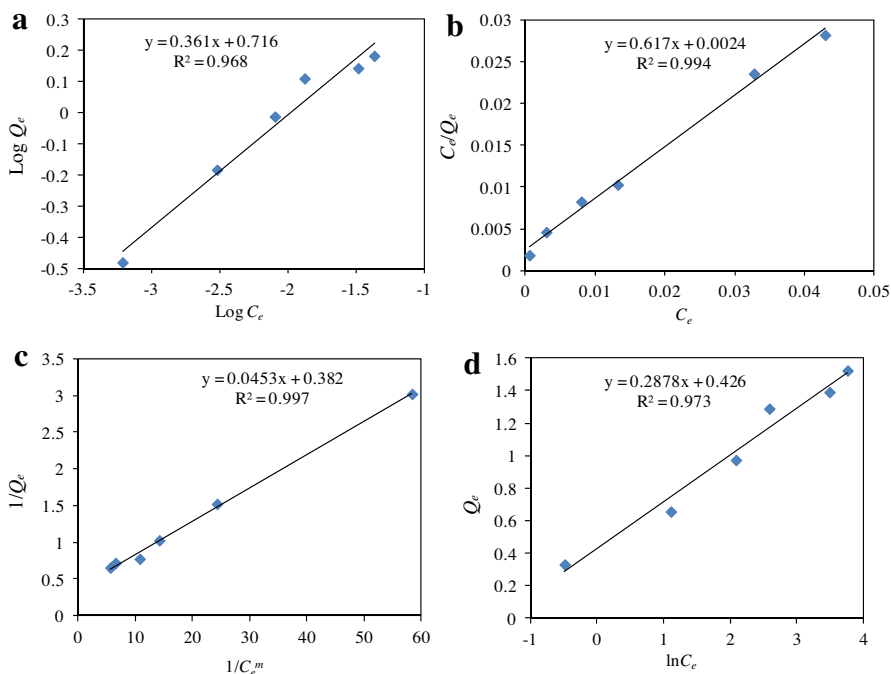


Fig. 6. (a) Freundlich isotherm illustrating the linear dependence of $\log q_e$ on $\log C_e$, (b) Langmuir isotherm illustrating the linear dependence of C_e/Q_e on C_e , (c) L–F isotherm illustrating the linear dependence of $1/Q_e$ on $1/C_e^m$, (d) Temkin isotherm illustrating the linear dependence of Q_e on $\ln C_e$.

of b and Q_m are determined from the plot of C_e/Q_e vs. C_e (Fig. 6b). Q_m is 1.62 mg g^{-1} , and b is 257.2 L mg^{-1} .

A dimensionless constant separation factor, r , is proposed to predict whether a Langmuir adsorption system is favorable or not. The type of favorability of the absorption isotherm is defined for specific r values as follows, for $r > 1$ unfavorable, $r = 1$ is linear, r between 0 and 1 is favorable and $r = 0$ irreversible [27]. The separation factor, r , is defined as follow:

$$r = 1/(1 + bC_0) \quad (9)$$

where C_0 is the initial concentration of chromium and b is the Langmuir adsorption constant (L mg^{-1}). Since both b and C_0 are greater than 0 in this study, the value of r lies within the range 0–1. This indicates the adsorption of Cr(VI) on maghemite particle is highly favorable under the experimental condition used in this study.

Standard Gibbs free energy (ΔG_0 , J mol^{-1}) can be used to evaluate the spontaneity of an adsorption process. A negative ΔG_0 indicates the adsorption occurs spontaneously and is thermodynamically stable, whereas the positive ΔG_0 means this process is a disfavored nonspontaneous reaction. The standard Gibbs free energy equation is expressed as following [28]:

$$\ln(1/b) = \Delta G_0/RT \quad (10)$$

where R is the ideal gas constant ($8.314 \text{ J K}^{-1} \text{ mol}^{-1}$) and T is absolute temperature (K). Since b is 257.2 L mg^{-1} , ΔG_0 is negative in this study. The result indicates that the adsorption process is spontaneous.

L–F isotherm is the combination of Langmuir and Freundlich isotherms [29]. The experimental data were also modeled with L–F adsorption isotherm.

$$Q_e = Q_m k C_e^m / (1 + k C_e^m) \quad (11)$$

where Q_m is the total amount of binding sites on the adsorbent surface, k is related to the mean association constant (K_0), $K_0 = k^{1/m}$, and m represents the heterogeneity index of the binding site energy, which varies from 0 to 1. As m approaches to 1, the adsorbent is homogeneous and the L–F equation is reduced to Langmuir iso-

therm. For a heterogeneous material, $m < 1$, and when either m or k is 0, the L–F equation can be reduced to Freundlich. Therefore, L–F isotherm is able to model both of homogeneous and heterogeneous adsorption systems. The maximum of R^2 is obtained from the plot of $1/Q_e$ vs. $1/C_e^m$ (Fig. 6c) by solver function of Microsoft Excel 2007, where $m = 0.55$. Therefore, the value of Q_m is 2.62 mg g^{-1} , and k is equal to 8.42 mg^{-1} . The mean association constant is 48.3 mg^{-1} .

The Temkin isotherm equation is given as [30]:

$$Q_e = (RT/b_i) \ln K_t + (RT/b_i) \ln C_e \quad (12)$$

where K_t is the Temkin isotherm constant (L g^{-1}), b_i is the Temkin constant related to heat of sorption (J mol^{-1}), R is the ideal gas constant ($8.314 \text{ J K}^{-1} \text{ mol}^{-1}$) and T is the Kelvin temperature (K). The value of K_t and b_i were obtained by the plotting of Q_e vs. $\ln C_e$ (Fig. 6d). K_t is 4.39 L g^{-1} , while b_i is 8.64 kJ mol^{-1} .

A comparison of R^2 was made among four adsorption isotherms. Compared to Langmuir, Freundlich and Temkin adsorption isotherms, L–F isotherm has the highest value of R^2 , indicating the adsorption of chromium by maghemite fits better with L–F isotherm. The heterogeneity index of L–F isotherm is 0.55, which is between 0 and 1. The adsorption has partial adsorption characteristics of Langmuir and Freundlich models. The adsorption fits also the Langmuir model nicely, and it may be due to monolayer adsorption. Therefore, adsorption isotherm studies imply that it is a heterogeneous monolayer adsorption [31].

3.6. The effect of pH on Cr(VI) adsorption

The pH effect on Cr(VI) adsorption was evaluated over a pH range from 2 to 10. HNO_3 and NaOH solutions were used to adjust solution pH. Fig. 7 shows the Cr(VI) removal as a function of pH. Electrostatic interactions can have a pronounced impact on adsorption processes. The $\text{p}K_{a1}$ and $\text{p}K_{a2}$ of chromic acid are 0.74 and 6.50, respectively. The zero point of charge (ZPC) of maghemite is 6.6 [16]. Below the pH of the ZPC the particle surface becomes positively charged, while Cr(VI) exists predominantly in dianionic

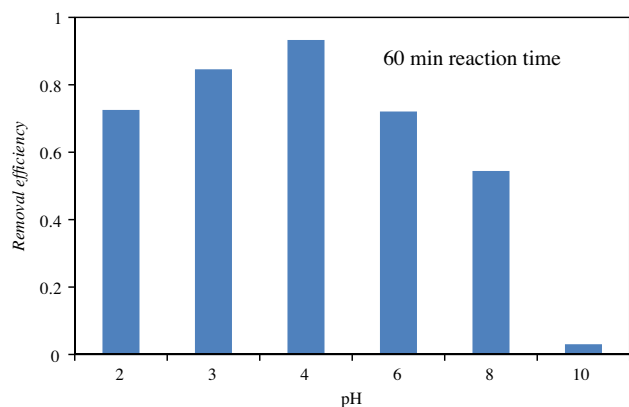


Fig. 7. Effect of pH on Cr(VI) adsorption. $[\text{Cr(VI)}]_0 = 500$ ppb, $[\text{maghemite}] = 0.3$ g/L.

(CrO_4^{2-}) and mono-anionic (HCrO_4^-) forms between pH ~ 2 and 6.5. Thus under mildly acidic conditions, attractive electrostatic interactions between negatively charged Cr(VI) species and the positive surface lead to favorable adsorption. We observed the removal efficiency of Cr(VI) increases with the decrease of pH to 4. However under strongly acidic conditions the adsorption decreases modestly as the Cr(VI) speciation becomes dominated by the neutral form (H_2CrO_4) eliminating the strong electrostatic attraction of negatively charged chromate species and positively charged surface. Above the pH of ZPC, the particle surface processes an overall negative charge while the dominant species of Cr(VI) is CrO_4^{2-} [32] and thus under basic conditions electrostatic repulsion exists and poor adsorption is observed. While pH can have a pronounced influence on the adsorption, effective removal can be achieved over a significant pH range from 2 to 8.

3.7. Effect of humic acid

The presence of humic acids in surface waters can have a pronounced effect on iron based water treatment processes [33]. Humic acids contain carboxylic acid and phenolic functional groups which can engage in ligand exchange and complexation of metal ions [34]. The adsorption of Cr(VI) by nanoparticles as a function of humic acid concentration is illustrated in Fig. 8. The interaction of humic acid with iron oxides can alter the surface property of

maghemite nanoparticles and the subsequent adsorption of Cr(VI). In the presence of 1 ppm humic acid we observed minimal change in the overall adsorption of Cr(VI). Under such conditions stabilization of the suspension leading to inhibition of particle aggregation, reduction of Cr(VI) [35], and humic acid complexation of chromate species can contribute to the removal of Cr(VI) [36]. At intermediate humic acid concentrations the observed Cr(VI) adsorption also does not change significantly. However as the concentration of humic acid increases the Cr(VI) adsorption decreases under our experimental conditions. The coating of maghemite nanoparticles with humic acid will increase with humic acid blocking potential adsorption sites for Cr(VI) and increasing the presence of negatively charged carboxylic groups at the surface essentially decreasing the ZPC of the particles [37]. Under these conditions repulsion will increase between negatively charged Cr(VI) and negatively charged humic acid modified surface. At high humic acid concentrations Cr(VI) adsorption decreased significantly possibly due to humic acid coating the as the iron oxide particle [38]. The removal of Cr(VI) can be achieved in the presence of significant levels of humic acid.

4. Conclusion

Magnetic maghemite nanoparticles were synthesized by a coprecipitation method, characterized and employed for Cr(VI) removal. The adsorption kinetics for Cr(VI) are accurately modeled by a pseudo-second-order model. The intraparticle diffusion model implies that the adsorption was controlled by surface sorption and intraparticle diffusion, followed by a redox reaction. The adsorption isotherm fits the L-F and Langmuir equations well implying heterogeneous monolayer adsorption. The standard Gibbs free energy, adsorption characteristics and effect of separation factor on isotherm shape indicate that adsorption of Cr(VI) is spontaneous, favorable and practical. The adsorption under basic condition is weak, but strong under the mildly acidic and neutral conditions often associated with contaminated surface waters. The presence of low concentrations of humic acid does not have a significant impact on the adsorption of Cr(VI) however at relatively high humic acid concentration (20 ppm) the adsorption of Cr(VI) can be partially inhibited. The maghemite nanoparticles are low-cost, easily prepared, magnetic, and good adsorbents for Cr(VI) making them a promising material for removal of Cr(VI) from aqueous solution.

Acknowledgments

KEO and DDD gratefully acknowledge NSF support (CBET033317). MHE acknowledges Ferdowsi University of Mashhad for financial support during the sabbatical in FIU. The authors greatly appreciate the constructive and insightful suggestions provided by the reviewers of our paper.

References

- [1] J. Johnson, L. Schewel, T.E. Graedel, The contemporary anthropogenic chromium cycle, *Environ. Sci. Technol.* 40 (2006) 7060–7069.
- [2] W. Mertz, Chromium in human nutrition: a review, *J. Nutr.* 123 (1993) 626–633.
- [3] M. Pérez-Candela, J. Martín-Martínez, R. Torregrosa-Maciá, Chromium(VI) removal with activated carbons, *Water Res.* 29 (1995) 2174–2180.
- [4] G. Quievryn, J. Messer, A. Zhitkovich, Carcinogenic chromium(VI) induces cross-linking of vitamin C to DNA in vitro and in human lung A549 cells, *Biochemistry* 41 (2002) 3156–3167.
- [5] D.H. Thomas, J.S. Rohrer, P.E. Jackson, T. Pak, J.N. Scott, Determination of hexavalent chromium at the level of the California Public Health Goal by ion chromatography, *J. Chromatogr. A* 956 (2002) 255–259.
- [6] H.M. Pouran, A. Fotovat, G. Haghnia, A. Halajnia, M. Chamsaz, A case study: chromium concentration and its species in a calcareous soil affected by leather industries effluents, *World Appl. Sci. J.* 5 (2008) 484–489.

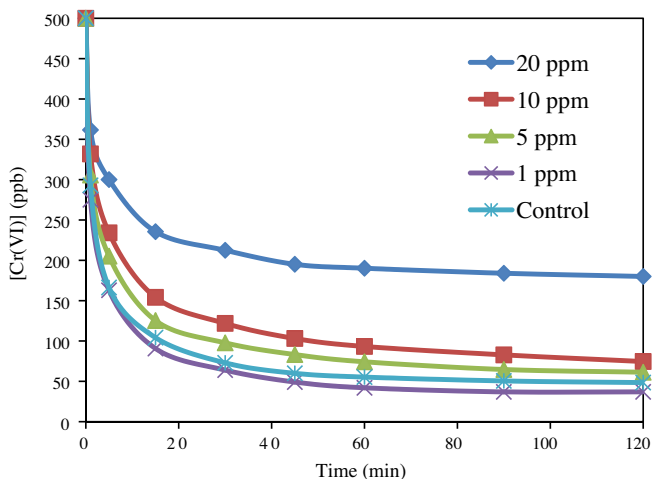


Fig. 8. Effect of humic acid on Cr(VI) adsorption. $[\text{Cr(VI)}]_0 = 500$ ppb, $[\text{maghemite}] = 0.3$ g/L.

- [7] M. Owlad, M.K. Aroua, W.A.W. Daud, S. Baroutian, Removal of hexavalent chromium-contaminated water and wastewater: a review, *Water Air Soil Pollut.* 200 (2009) 59–77.
- [8] S.S. Banerjee, D. Chen, Fast removal of copper ions by gum Arabic modified magnetic nano-adsorbent, *J. Hazard. Mater.* 147 (2007) 792–799.
- [9] J. Hu, I.M.C. Lo, G. Chen, Comparative study of various magnetic nanoparticles for Cr(VI) removal, *Sep. Purif. Technol.* 56 (2007) 249–256.
- [10] J. Hu, I.M.C. Lo, G. Chen, Removal of Cr(VI) by magnetite nanoparticles, *Water Sci. Technol.* 50 (2004) 139–146.
- [11] C.T. Yavuz, J.T. Mayo, W.W. Yu, A. Prakash, J.C. Falkner, S. Yean, L. Cong, H.J. Shipley, A. Kan, M. Tomson, D. Natelson, V.L. Colvin, Low-field magnetic separation of monodisperse Fe₃O₄ nanocrystals, *Science* 314 (2006) 964–967.
- [12] S.R. Chowdhury, E.K. Yanful, Arsenic and chromium removal by mixed magnetite–maghemite nanoparticles and the effect of phosphate on removal, *J. Environ. Manage.* 91 (2010) 2238–2247.
- [13] S. Lin, D. Liu, Z. Liu, Removal of arsenic contaminants with magnetic γ -Fe₂O₃ nanoparticles, *Chem. Eng. J.* 211–212 (2012) 46–52.
- [14] A. Roy, J. Bhattacharya, Removal of Cu(II), Zn(II) and Pb(II) from water using microwave-assisted synthesized maghemite nanotubes, *Chem. Eng. J.* 211–212 (2012) 493–500.
- [15] E. Darezereshki, M. Ranjbar, F. Bakhtiari, One-step synthesis of maghemite (γ -Fe₂O₃) nano-particles by wet chemical method, *J. Alloys Comp.* 502 (2010) 257–260.
- [16] R.M. Cornell, U. Schwertmann, *The Iron Oxides: Structure, Properties, Reactions, Occurrences and Uses, Completely Revised and Extended*, second ed., Wiley-Vch, Weinheim, 2003.
- [17] S. Gota, E. Guio, M. Henriot, M. Gautier-Soyer, Atomic-oxygen-assisted MBE growth of α -Fe₂O₃ on α -Al₂O₃(0001): Metastable FeO(111)-like phase at subnanometer thicknesses, *Phys. Rev. B* 60 (1999) 14387–14395.
- [18] P. Li, E.Y. Jiang, H.L. Bai, Fabrication of ultrathin epitaxial γ -Fe₂O₃ films by reactive sputtering, *J. Phys. D: Appl. Phys.* 44 (2011) 075003.
- [19] A.P. Grosvenor, B.A. Kobe, M.C. Biesinger, N.S. McIntyre, Investigation of multiplet splitting of Fe2p XPS spectra and bonding in iron compounds, *Surf. Interface Anal.* 36 (2004) 1564–1574.
- [20] P. Yuan, D. Liu, M. Fan, D. Yang, R. Zhu, F. Ge, J. Zhu, H. He, Removal of hexavalent chromium [Cr(VI)] from aqueous solutions by the diatomite-supported/unsupported magnetite nanoparticles, *J. Hazard. Mater.* 173 (2010) 614–621.
- [21] A.E. Ofomaja, Kinetics and mechanism of methylene blue sorption onto palm kernel fibre, *Process. Biochem.* 42 (2007) 16–24.
- [22] I.D. Mall, V.C. Srivastava, N.K. Agarwal, Removal of orange-G and methyl violet dyes by adsorption onto bagasse fly ash – kinetic study and equilibrium isotherm analyses, *Dyes. Pigments.* 69 (2006) 210–223.
- [23] B.H. Hameed, J.M. Salman, A.L. Ahmad, Adsorption isotherm and kinetic modeling of 2,4-D pesticide on activated carbon derived from date stones, *J. Hazard. Mater.* 163 (2008) 121–126.
- [24] S.K. Singh, T.G. Townsend, D. Mazyck, T.H. Boyer, Equilibrium and intraparticle diffusion of stabilized landfill leachate onto micro- and meso-porous activated carbon, *Water Res.* 46 (2012) 491–499.
- [25] B.E. Reed, M.R. Matsumoto, Modeling cadmium adsorption by activated carbon using the Langmuir and Freundlich isotherm expressions, *Sep. Sci. Technol.* 28 (1993) 2179–2195.
- [26] R.E. Treybal, *Mass-Transfer Operation*, third ed., McGraw-Hill, Singapore, 1981.
- [27] W.S.W. Ngah, C.S. Endud, R. Mayanar, Removal of copper(II) ions from aqueous solution onto chitosan and cross-linked chitosan beads, *React. Funct. Polym.* 50 (2002) 181–190.
- [28] Y. Ho, A.E. Ofomaja, Kinetics and thermodynamics of lead ion sorption on palm kernel fibre from aqueous solution, *Process Biochem.* 40 (2005) 3455–3461.
- [29] R.J. Umpleby, S.C. Baxter, Y. Chen, R.N. Shah, K.D. Shimizu, Characterization of molecularly imprinted polymers with the Langmuir–Freundlich Isotherm, *Anal. Chem.* 73 (2001) 4584–4591.
- [30] M. Özacar, I.A. Sengil, Adsorption of metal complex dyes from aqueous solutions by pine sawdust, *Bioresour. Technol.* 96 (2005) 791–795.
- [31] C.K. Lee, K.S. Low, K.L. Kek, Removal of chromium from aqueous solution, *Bioresour. Technol.* 54 (1995) 183–189.
- [32] R.K. Tandon, P.T. Crisp, J. Ellis, Effect of pH on Chromium(VI) species in solution, *Talanta* 31 (1984) 227–228.
- [33] B. Gu, J. Schmitt, Z. Chen, L. Liang, J.F. McCarthy, Adsorption and desorption of natural organic matter on iron oxide: mechanisms and models, *Environ. Sci. Technol.* 28 (1994) 38–46.
- [34] A.W.P. Vermeer, J.K. McCulloch, W.H. van Riemsdijk, L.K. Koopal, Metal ion adsorption to complexes of humic acid and metal oxides: deviations from the additivity rule, *Environ. Sci. Technol.* 33 (1999) 3892–3897.
- [35] P.R. Wittbrodt, C.D. Palmer, Reduction of Cr(VI) in the presence of excess soil fulvic acid, *Environ. Sci. Technol.* 29 (1995) 255–263.
- [36] C.S. Uyguner, M. Bekbolet, Evaluation of humic acid, Chromium(VI) and TiO₂ ternary system in relation to adsorption interactions, *Appl. Catal. B* 49 (2004) 267–275.
- [37] E. Illés, E. Tombácz, The role of variable surface charge and surface complexation in the adsorption of humic acid on magnetite, *Colloids Surf. A* 230 (2004) 99–109.
- [38] J.-D. Hu, Y. Zevi, X.-M. Kou, J. Xiao, X.-J. Wang, Y. Jin, Effect of dissolved organic matter on the stability of magnetic nanoparticles under different pH and ionic strength conditions, *Sci. Total. Environ.* 408 (2010) 3477–3489.